Effect of Nucleation Profile on Particle-Size Distribution

A. N. Sathyagal and A. V. McCormick
Dept. of Chemical Engineering and Materials Science, University of Minnesota, Minneapolis, MN 55455

Nucleation transients are important features in the reactive generation of monodisperse colloids from solution. Many previous theoretical investigations, both analytical and numerical, have addressed the roles of colloid aggregation or of direct growth from solution. Few have addressed the role of nucleation transients on the size distribution. The population balance model was used to study the effect of nucleation transients on an aggregating colloidal dispersion. (To simplify the problem, growth was neglected.) The focus was on whether, under the action of aggregation alone, extended and divided nucleation periods in some cases can lead to a very narrow particle-size distribution. Our results support previous treatments (Look et al., 1990; Bogush and Zukoski, 1991b) suggesting this is the case. Our general approach also offers additional insights, such as strategies to manipulate the nucleation transients to independently tune the average particle size and the variance of the distribution.

Introduction

The solution synthesis of monodisperse colloids is important from both a fundamental perspective (such as model systems to study surface forces and test condensed matter theory) and for practical applications (such as to provide new materials for ceramic green bodies). Most techniques to synthesize monodisperse colloids in batch or plug-flow reactors (including emulsion and dispersion polymerization, hydrolysis/condensational precipitation of metal alkoxides and salts) involve the interplay of (1) nucleation of insoluble reaction products from solution, (2) aggregation of the resulting particles and/or droplets, and, (3) sometimes, direct growth of particles by addition of soluble species. (In the remainder of this article, "growth" will be defined strictly in this way.)

There has been some controversy in the literature regarding the role of and transients in nucleation in batch reactors and the subsequent roles that aggregation and growth play, individually and coupled, that can lead to monodisperse colloids. The Stöber synthesis of silica colloids can serve as an example. In their original model for the formation of monodisperse sols, LaMer and Dinegar (1950) surmised that the monodispersity was due to a short burst of nucleation followed by growth of the nucleated particles by the continued addition of insoluble reaction products. Some researchers have found this concept useful in analyzing the Stöber process (Matsoukas and Gulari, 1988, 1989, 1991). On the other hand, several authors have shown experimental evidence for continuous nucleation during the batch Stöber process (Bogush and Zukoski, 1991a,b; Lee et al., 1997). Moreover, some suggest that aggregation alone might lead to the monodisperse product, given the high probability of aggregation between a small nucleus and a large aggregate (Bogush and Zukoski, 1991a,b).

In this article, we will use the population balance model to examine the coupled influence of nucleation and aggregation transients (neglecting growth for the moment). Numerous analytical and numerical studies have addressed the effects of aggregation, breakage and growth on the size distribution (reviewed by Ramkrishna (1985)). Less attention has been paid to the effect of time dependence of nucleation (the "nucleation profile"). Still, there are some excellent leads (as discussed below). We extend these treatments to address how the nucleation profile affects the evolving particle-size distribution. First, we generalize the model used by Zukoski and coworkers (Bogush and Zukoski, 1991b; Look et al., 1990) to further explain their colloid synthesis experimental results.

Correspondence concerning this article should be addressed to A. V. McCormick.

We will investigate the problem under the influence both of Brownian aggregation and of "DLVO aggregation" (by which we mean Brownian aggregation modified by the effects of van der Waals attraction and electrostatic repulsion).

Next, we explore finite nucleation periods (at varying rates) and a double nucleation period. The latter simulates what happens if more material is added to a semibatch reactor.

In all cases, we will have *no* particles present initially; particles will be generated only by nucleation. We recognize that surface nucleation and particle growth no doubt also play a role, especially late in the reaction. However, we neglect these processes in this analysis to study if aggregation alone can generate a monodisperse distribution in a nucleating system. In our analysis, we also assume that aggregation results in compact, spherical particles (the aggregating entities can rearrange to minimize interfacial area). This allows us to use the expressions developed for the interaction potential between two spherical particles. Our results, hence, do not apply to fractal structures.

Previous Population Balance Treatments

The population balance approach accounts for all processes which change the state of a particle in a dispersion and has been reviewed by Ramkrishna (1985). Here, we highlight only those equations and references immediately relevant to the problem at hand. For a dispersion undergoing nucleation (assuming all nuclei are of the same size) and aggregation alone, the population balance equation is given by

$$\frac{\partial n(v,t)}{\partial t} = J(t)\delta(v - v_0) + \frac{1}{2}\int_0^v q(v-v', v')n(v-v',t)n(v',t)dv' - \int_0^\infty q(v,v')n(v,t)n(v',t)dv' \quad (1)$$

where $n(v,t)$ is the number density of particles in the volume range $(v, v+dv)$, $J(t)$ is the nucleation rate (with nucleus volume v_0) and $q(v,v')$ is the aggregation rate of particles of volumes v and v'. The equation is made dimensionless by scaling with respect to a characteristic volume v_0 and a characteristic time v_0/q_0. The characteristic aggregation rate is $q_0 = 8kT/3\mu$, where k is Boltzmann's constant, T is the temperature, and μ is the viscosity of the continuous phase. The dimensionless equation is

$$\frac{\partial \tilde{n}(\tilde{v},\tau)}{\partial \tau} = \sigma\delta(\tilde{v}-1) + \frac{1}{2}\int_0^{\tilde{v}} \tilde{q}(\tilde{v}-\tilde{v}',\tilde{v}')\tilde{n}(\tilde{v}-\tilde{v}',\tau)\tilde{n}(\tilde{v}',\tau)d\tilde{v}' - \int_0^\infty \tilde{q}(\tilde{v},\tilde{v}')\tilde{n}(\tilde{v},\tau)\tilde{n}(\tilde{v}',\tau)d\tilde{v}' \quad (2)$$

where

$$\tilde{v} = v/v_0$$

$$\tau = q_0 t/v_0$$

$$\tilde{q}(\tilde{v},\tilde{v}') = \frac{q(v,v')}{q_0}$$

$$\tilde{n}(\tilde{v},\tau) = v_0^2 n(v,t)$$

$$\sigma = \frac{v_0^2 S(t)}{q_0}$$

We will present results for the various cases considered in this study in the form of the volume fraction density distribution $\tilde{f}(\tilde{v},\tau) = \tilde{v}\tilde{n}(\tilde{v},\tau)$ vs. particle volume $\tilde{v}$. Following Ramkrishna et al. (1995), we believe the volume fraction density distribution provides a better description of dispersed-phase systems than does the number density distribution because the volume fraction density distribution naturally weights the different-sized particles of the dispersed phase according to their contribution to the overall process.

There have been many studies in the aerosol literature on the effects of various combinations of aggregation, growth, evaporation, and nucleation processes on the particle-size distribution (see, for example, the works of Ramabhadran et al., 1976; McMurry and Friedlander, 1979; Gelbard and Seinfeld, 1979a,b; McMurry, 1983; Warren and Seinfeld, 1984). Most of these studies did not include the effects of interparticle forces and temporal nucleation profile on the size distribution.

Analytical solutions to Eq. 2 are elusive even for simple forms of the aggregation and nucleation rates. Peterson et al. (1978) and Gelbard and Seinfeld (1978) have solved a form of Eq. 2 numerically (also including other terms for particle growth and removal) for the case of a suspension with a specific initial distribution of particle sizes (an exponential distribution). They nucleated particles (of various sizes) at a constant rate and all particles aggregated at a rate given by $\tilde{q}(\tilde{v},\tilde{v}') \propto (\tilde{v}+\tilde{v}')$, or $\tilde{q}(\tilde{v},\tilde{v}') = K$, a constant. Rao and McMurry (1989) have solved Eq. 2 for the case of an aerosol with no initial particles, constant source (or nucleation) rate, and a free molecular Brownian aggregation rate. They also included the effects of a van der Waals attraction force and monomer evaporation in some cases. Quon and Mockros (1965) and Mockros et al. (1967) used the discrete version of Eq. 2 for the case of no initial particles and for a constant nucleation rate with two different types of aggregation rate $\tilde{q}(\tilde{v},\tilde{v}')$: (1) one which is constant and independent of particle size; and (2) one which is dependent on the particle size and is due to the Brownian motion of the particles. In both cases, they showed that the number density distribution $\tilde{n}(\tilde{v},\tau)$ reaches a steady state (scaled with respect to a factor proportional to N_s^2, where N_s is the total particle number density at steady state) identically for these two cases. We will have the opportunity to confirm this result for Brownian aggregation and to incorporate the effects of interparticle forces on the particle aggregation rate. More importantly, we will investigate different nucleation profiles.

Zukoski and co-workers have solved the population balance equation numerically for the specific cases of silica (Bogush and Zukoski, 1991b) and titania (Look et al., 1990)

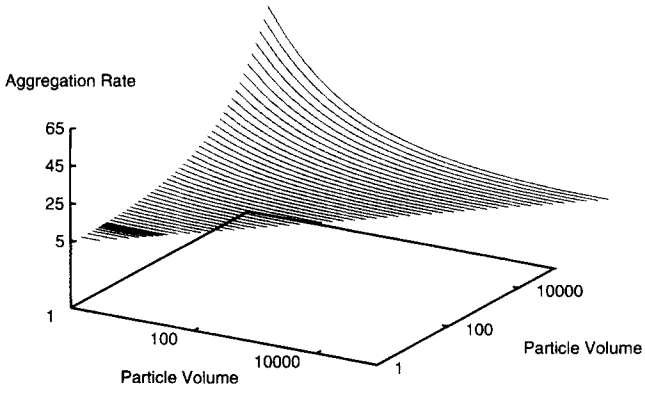

Figure 1. Brownian aggregation frequency as a function of particle pairs.

colloid syntheses. They report the evolution of the total particle number under the influence of a nucleation profile that is suggested experimentally by the disappearance of dissolved monomer. This article serves as a generalization of this type of analysis. We will investigate the effects of different generic nucleation rates and profiles on the particle-size distribution. However, whereas Zukoski and co-workers accounted for interparticle van der Waals, electrostatic, and solvation forces, we will omit solvation forces in the interest of generality.

Models for Aggregation

Brownian aggregation kernel

In a quiescent reaction medium, particles move in random Brownian fashion. Two such particles will aggregate when they come very close to one another. When there are no attractive or repulsive forces between the particles, they must simply touch; the aggregation rate then is given by the Brownian aggregation kernel (Smoluchowski, 1916)

$$q(v,\tilde{v}) = K(v^{1/3} + v'^{1/3})(v^{-1/3} + v'^{-1/3}) \tag{3}$$

where K is a constant related to the viscosity of the suspending medium and the temperature.

Figure 1 shows the Brownian aggregation rate as a function of the particle pairs undergoing aggregation. It shows that the aggregation rate for two equal sized particles is independent of the particle size. Dissimilar particles have a higher rate than equal sized particles; the greater the dissimilarity in size between the two particles, the higher the aggregation rate. Even so, the magnitude of the aggregation rate function does not change dramatically with the particle volumes in comparison with the following.

"DLVO" aggregation kernel

In solution, colloidal particles will have attractive and repulsive forces between one another. In such a case, the above Brownian aggregation rate is scaled by a stability factor (Verwey and Overbeek, 1948), that is,

$$q(v,v') = q_B(v,v')/W(v,v') \tag{4}$$

where $q_B(v,v')$ is the aggregation rate given by Eq. 3. $W(v,v')$ is the stability factor which depends on the particle sizes and is related to the interaction potential energy V_T between the particles through the following equation

$$W(v,v') = 2\int_0^\infty \frac{\exp[V_T(x;v,v')/kT]}{(x+2)^2}\,dx \tag{5}$$

where k is Boltzmann's constant, T is the temperature, and x is the shortest scaled distance between the particle surfaces. The interaction energy V_T is the sum of all the attractive and repulsive interactions between the particles. This definition of the stability factor assumes that aggregation occurs only when the two particles have overcome the repulsive energy barrier and are at the primary minimum in the interaction energy curve; we will neglect "weak" aggregation in the secondary minimum.

We will only consider the effects of van der Waals attractive forces and electrostatic repulsive forces between the particles

$$V_T = V_{vdw} + V_{elec} \tag{6}$$

Assuming the particles are spherical, the van der Waals attractive interaction potential energy between two particles of radius a_1 and a_2 is given by (Hamaker, 1937)

$$V_{vdw} = -\frac{A_H}{6}\left[\frac{2a_1a_2}{R^2-(a_1-a_2)^2} + \frac{2a_1a_2}{R^2-(a_1-a_2)^2} + \ln\frac{R^2-(a_1+a_2)^2}{R^2-(a_1-a_2)^2}\right] \tag{7}$$

where A_H is the Hamaker constant and R is the distance between the centers of the two particles.

Many studies to determine the electrostatic interaction between two spherical particles use the linearized form of the Poisson-Boltzmann equation to obtain approximate expressions for the electrostatic interaction potential. The nature of the approximations involved in the derivations limits the validity of each expression to certain ranges of the experimental variables. We will use two of these, where both expressions assume that the surface potential is independent of size and remains constant as the particles approach:

(1) For $\kappa a < 5$ (where κ is the inverse Debye length and a is the particle radius), we will use the linear superposition approximation (LSA) expression given by Ohshima (1995)

$$V_{elec} = 4\pi\epsilon a_1a_2Y_1Y_2\left(\frac{kT}{e}\right)^2\frac{\exp(-\kappa x)}{x+a_1+a_2} \tag{8}$$

where

$$Y_i = \frac{8\tanh(e\psi_0/4kT)}{1+\left[1-\frac{2\kappa a_i+1}{(\kappa a_i+1)^2}\tanh^2(e\psi_0/4kT)\right]^{1/2}} \tag{9}$$

ϵ is the dielectric constant of the suspension medium, ψ_0 is the surface potential, x is the closest distance between the particle surfaces, k is Boltzmann's constant, T is the absolute temperature and e is the electronic charge;

(2) For $\kappa a > 5$, we will use the Hogg-Healy-Fuerstenau result (1966)

$$V_{\text{elec}} = 4\pi\epsilon\psi_0^2 \frac{a_1 a_2}{a_1 + a_2} \ln[1 + \exp(-\kappa x)] \qquad (10)$$

For typical values of the parameters of Eqs. 7, 8 and 10, Figure 2 shows the total interaction potential as a function of interparticle distance for three different particle pairs. The parameter values used in these calculations are: $\psi_0 = 50$ mV, $\kappa = 2\times10^8$ m^{-1}, $\epsilon = 7.0832\times10^{-10}$ C/V·m, $A_H = 1\times10^{-19}$ J. The particle sizes used in these calculations are $a_1 = 2\times10^{-9}$ m, and $a_2 = 4\times10^{-8}$ m. This a_1 value is also used as the size of the nucleating species in all the calculations presented in this article. The repulsive electrostatic interaction is dominant, leading to a maximum of large magnitude in V_T for the particle pairs shown in the figure. This maximum leads to a large value of the stability factor $W(v, v')$, and significantly reduces the aggregation rate of the particles. However, the figure also shows that the magnitude of the maximum is much larger for the interaction between two large particles compared to those for two small particles or one large and one small particle (the maxima in the latter two cases are similar in magnitude to one another). This indicates that the stability factor for the aggregation of two large particles is much higher than in the other two cases (note that the stability factor is related to the exponential of the potential). This means that in a dispersion containing a distribution of particle sizes, the large particles will preferentially aggregate with the small particles, while the small particles will aggregate with almost equal probability with all other particle sizes present in the system.

A plot of the aggregation frequency (calculated by including the stability factor) vs. the particle sizes is shown in Figure 3. Clearly, the dramatic increase in the stability factor for the aggregation of two comparably sized large particles leads to a very low aggregation rate for two large particles.

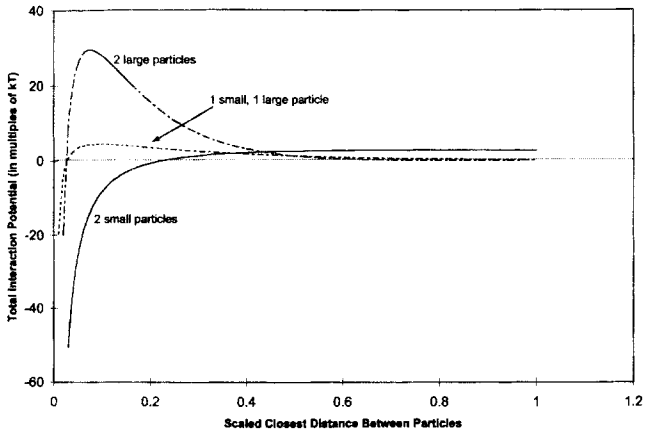

Figure 2. Total interparticle potential as a function of distance between particle surfaces.

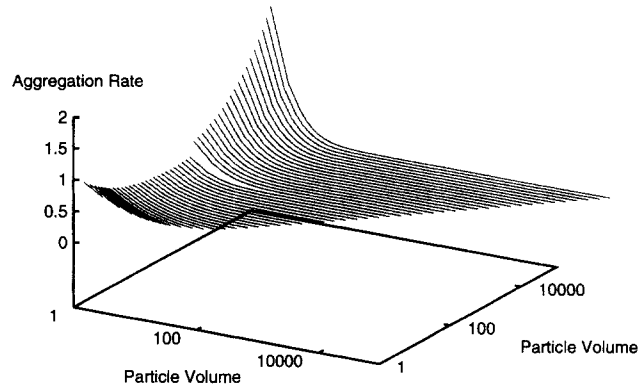

Figure 3. Particle aggregation frequencies with the inclusion of interparticle forces.

Computational Method

The discretization technique of Kumar and Ramkrishna (1996) is used to solve Eq. 2. The technique allows for an arbitrary discretization of the particle-size range. In this work, the particle-size range has been discretized as follows: A linear discretization for the first 10 particle sizes, followed by a geometric grid for the larger particle sizes with a constant ratio of 1.3 between adjacent discrete particle sizes. Fifty discrete sizes were typically used in the computations. This ensured a wide size range and, hence, no mass loss during the time scale of the computations.

A few simple measures of the particle-size distribution are also computed from the transient distributions. These measures are typically reported in the colloid synthesis literature and can give a reasonable description of the particle-size distribution for simple and sharp distributions. These include the total particle number density

$$N(\tau) = \int_0^\infty \tilde{n}(\tilde{v}, \tau)\, d\tilde{v} \qquad (11)$$

an average particle volume

$$\bar{v} = \frac{M_1}{M_0} \qquad (12)$$

and the normalized volume and diameter variances

$$\sigma_v^2 = \frac{M_2 M_0 - M_1^2}{M_1^2} \qquad (13)$$

and

$$\sigma_d^2 = \frac{M_{2/3} M_0 - M_{1/3}^2}{M_{1/3}^2} \qquad (14)$$

In Eqs. 12, 13, and 14, M_i is the i-th moment of the distribution defined by

$$M_i = \int_0^\infty \tilde{v}^i \tilde{n}(\tilde{v}, \tau)\, d\tilde{v} \qquad (15)$$

The normalized variances are commonly used in the monodispersed colloid synthesis literature to quantify the spread of the particle-size distribution.

The evolution of the total particle number density, $N(\tau)$, can be determined from Eq. 2 through

$$\frac{dN(\tau)}{d\tau} = \sigma - \frac{1}{2}\int_0^{\infty} d\tilde{v}\tilde{n}(\tilde{v},\tau)\int_0^{\infty}\tilde{q}(\tilde{v},\tilde{v}')\tilde{n}(\tilde{v}',\tau)d\tilde{v}' \quad (16)$$

Results and Discussion

Nucleation profiles

The effect of the nucleation profile is evaluated for three cases. First, the nucleation rate is held constant for the duration of the simulation ("continuous nucleation"), but we will vary this rate. Second, the nucleation rate is held constant for some time but then it is set to zero ("finite nucleation"); we will vary the duration of the nucleation period. Third, particles nucleate at a constant rate for some time; nucleation stops for some time; then nucleation begins anew at the former rate for some time ("double nucleation"). This is meant to simulate what happens in a semibatch reactor if more metastable material is added. We will study the effects of the start time and the duration of the second nucleation period.

Continuous nucleation

Brownian Aggregation. This first case has been investigated (Mockros et al., 1967), but it serves as a good introduction to our results and confirms our numerical method. Figure 4a shows the transient particle-size distributions (presented as volume fraction density distributions) for a system undergoing Brownian aggregation with a constant nucleation rate. A qualitative description of the evolution of the particle-size distribution is as follows. As nuclei establish higher concentrations, they begin to aggregate with one another to form larger particles. Somewhat later, the continually generated small particles aggregate with all other particles in the system. Owing both to their small number concentration and to their higher aggregation probability with small particles, the larger particles preferentially aggregate with the small particles. Since nucleation still proceeds, at some later point, a situation arises in which the rate of nucleation of the small particles balances the rate at which these particles aggregate. At this point, the concentration of small particles reaches a steady state.

For somewhat larger particle sizes, a similar approach to steady state can be envisioned at a somewhat later time. As the smaller particle sizes reach steady state, the rate of formation of larger particles by aggregation of the smaller particles will also reach a steady-state value. As their number concentration increases, their aggregation rate to form larger particles also increases. Eventually, a steady state will be reached for these somewhat larger particles as well. Hence, for a system undergoing Brownian aggregation with a constant nucleation rate, the transient particle-size distributions will show a steady-state region at the small particle size regime, with a gradual growth of the steady-state regime.

These results are identical to those of Mockros et al. (1967), and so they serve to show that the numerical scheme used here gives accurate results. As shown in the figure, the smallest particle sizes quickly reach a steady-state value. As aggregation proceeds, a larger range of particle sizes reaches a steady state and the distribution broadens to encompass a greater range of particle sizes.

Figure 4b shows the total number density $N(\tau)$, average size, and the normalized variances σ_v and σ_d as functions of time. $N(\tau)$ quickly reaches a constant value. This result, along with the transient particle-size distribution results, indicates that at late stages each newly nucleated particle in effect is incorporated (via aggregation) to the large-size end of the particle-size distribution. As a consequence of aggregation, the average particle size increases with time. The normalized variance increases continually with time, that is, there is a gradual broadening of the particle-size distribution. Similar results for the particle-size distribution and its various measures are obtained with other nucleation rates.

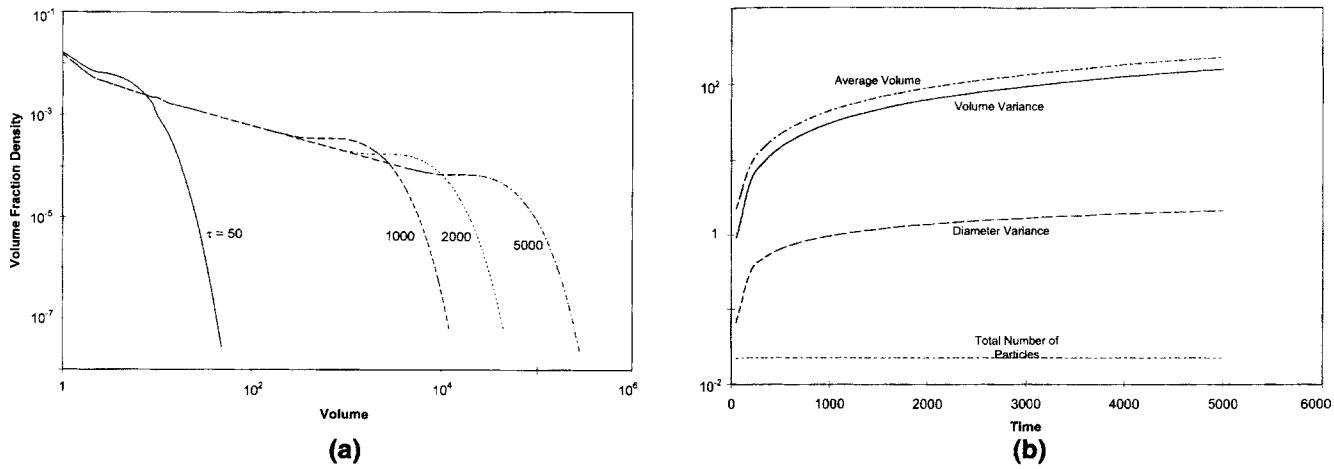

Figure 4. (a) Transient particle-size distributions, (b) simple measures of the distribution for a system with no initial particles, Brownian aggregation, and a constant nucleation rate, illustrating the steady state achieved in the distribution at the smaller particle volumes.

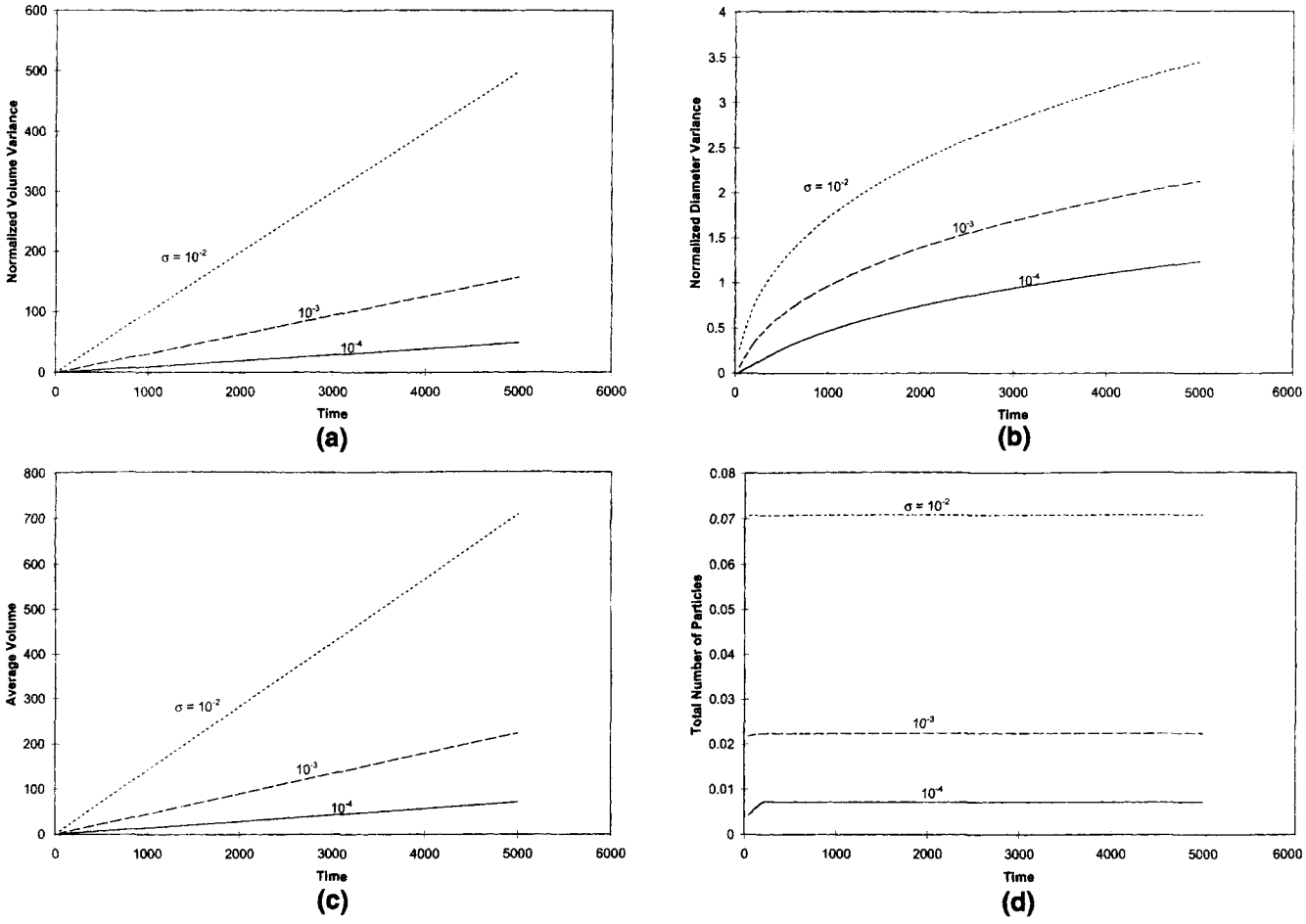

Figure 5. Evolution of the (a) normalized volume variance, (b) normalized diameter variance, (c) average volume, (d) total number of particles for a system with no initial particles, Brownian aggregation, and for different constant nucleation rates.

Larger nucleation rates lead to larger values of these simple measures of the size distribution.

Next, we will examine how the nucleation rate affects various simplistic measures of the size distribution. Figure 5 shows the effect of nucleation rate for a fixed aggregation rate function on the total number density, the average size, and the normalized variances. The total number density reaches a steady state earlier when the nucleation rate is higher. This is a consequence of the fact that the rate of depletion of the total particle number density is proportional to the square of the total particle number density. The higher nucleation rate increases the particle number density quickly, but this also sharply increases the depletion rate due to aggregation; hence, the total particle number density reaches the steady state in a shorter period of time. The steady-state value of the total number density, the average size, and the normalized variances increase with the nucleation rate.

Aggregation with Attractive and Repulsive Forces. The effect of nucleation on a system now undergoing "DLVO aggregation" with attractive and repulsive forces is shown in Figure 6a. As in the case of pure Brownian aggregation, one expects that the distribution would reach a steady state. However, the distribution has still not reached a steady state over the time scale of the simulation. DLVO interactions delay the steady state. Moreover, the nature of the distribution in this case is very different from the distribution seen in the case of Brownian aggregation. The distribution exhibits a peak with the location of the peak slowly increasing with time. There is a reasonably high concentration of the nucleating particles with only a slow decrease over time.

Interestingly, there is a negligible concentration of particles in the size range between the nuclei and the peak in the distribution. This becomes even more clear with a higher nucleation rate as shown in Figure 7a. Figures 6b and 7b show the evolution of the various measures of the distributions for these two cases. In each case, it is seen that the volume and diameter variances reach a peak value initially, but then slowly decrease with time. The total number density also goes through a peak value, but then very slowly decreases with time. The evolution of the particle-size distribution for these cases can be viewed almost as a growth process with freshly nucleated small particles adding to the large particles. (This may account for the differing explanations provided for the dominant processes present in the synthesis of Stöber silica spheres—some advocating growth, others advocating aggregation.)

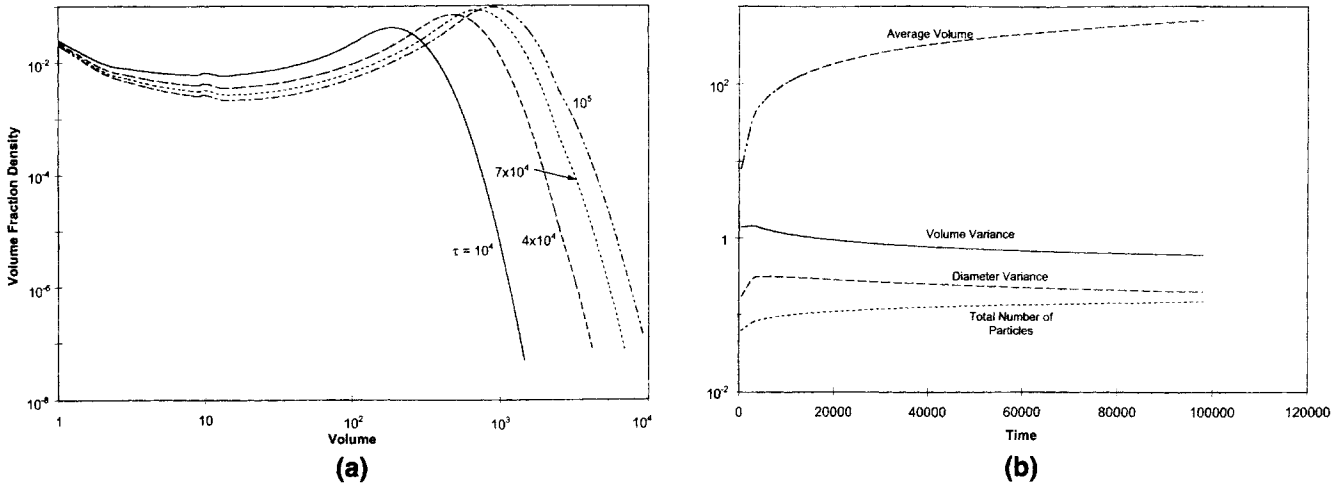

Figure 6. (a) Transient particle-size distributions; (b) simple measures of the distribution for a system with no initial particles, aggregation with DLVO interactions, and a constant nucleation rate $\sigma = 0.001$.

The evolution of the particle-size distribution can be explained by considering the shape of the aggregation frequency curve when attractive and repulsive forces are present. As shown in Figure 3, for a given particle size, the aggregation frequency goes through a minimum. As larger particles form, the small particles (close to the nucleate size) will preferentially aggregate with them. Since the aggregation rate of small particles with intermediate-sized particles goes through a minimum, the fraction of small particles aggregating with the intermediate-sized particles decreases. However, these intermediate-sized particles will still aggregate at a finite rate with the larger particles in the system, so intermediate particles get depleted.

The effect of a higher nucleation rate is to increase the formation rate of large particles and, hence, to increase the average particle size. Since these larger particles have a higher rate of aggregation with both the small nucleates and with the intermediate-sized particles, the intermediate-sized particles get depleted much faster at a higher nucleation rate. Since the rate of aggregation of two large particles is negligibly small, the distribution does not broaden rapidly as in the case of Brownian aggregation.

Finite nucleation

Brownian Aggregation. The effect of stopping nucleation on the particle-size distribution is shown in Figure 8a for particles without attraction or repulsion. The results are shown only for one value of the nucleation rate; similar results are obtained if other nucleation rates are used. While nucleation proceeds, the evolution of the particle-size distribution is identical to that discussed in the section on Brownian aggregation. Particles up to size 2 have reached a steady state at the time nucleation stops. The figure shows that after nucleation stops, the particle-size distribution continues to evolve,

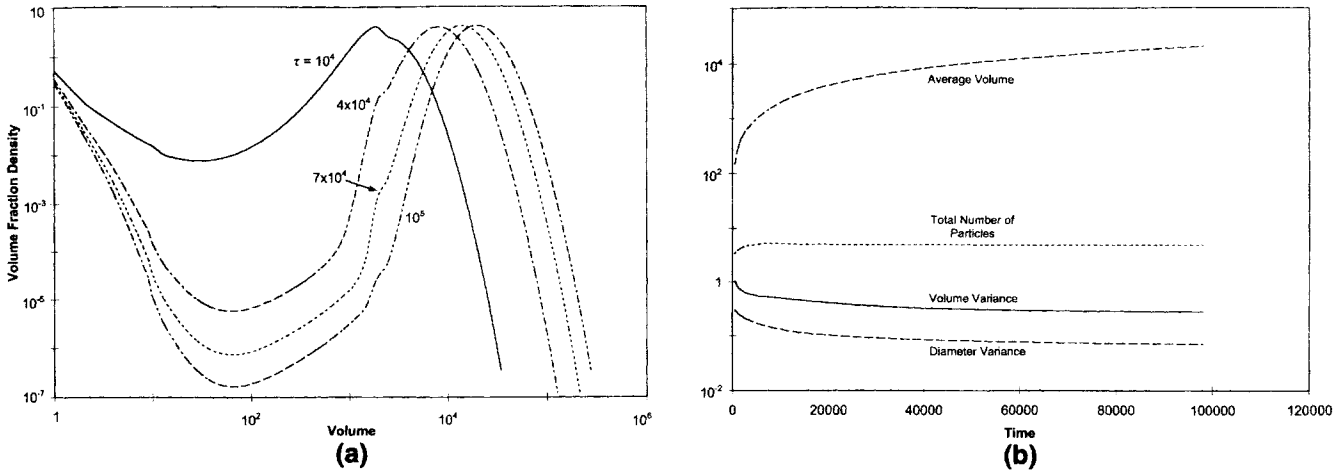

Figure 7. (a) Transient particle-size distributions, and (b) simple measures of the distribution for a system with no initial particles, aggregation with DLVO interactions, and a constant nucleation rate $\sigma = 1.0$.

Higher nucleation rates lead to sharper distributions (cf. Figure 6).

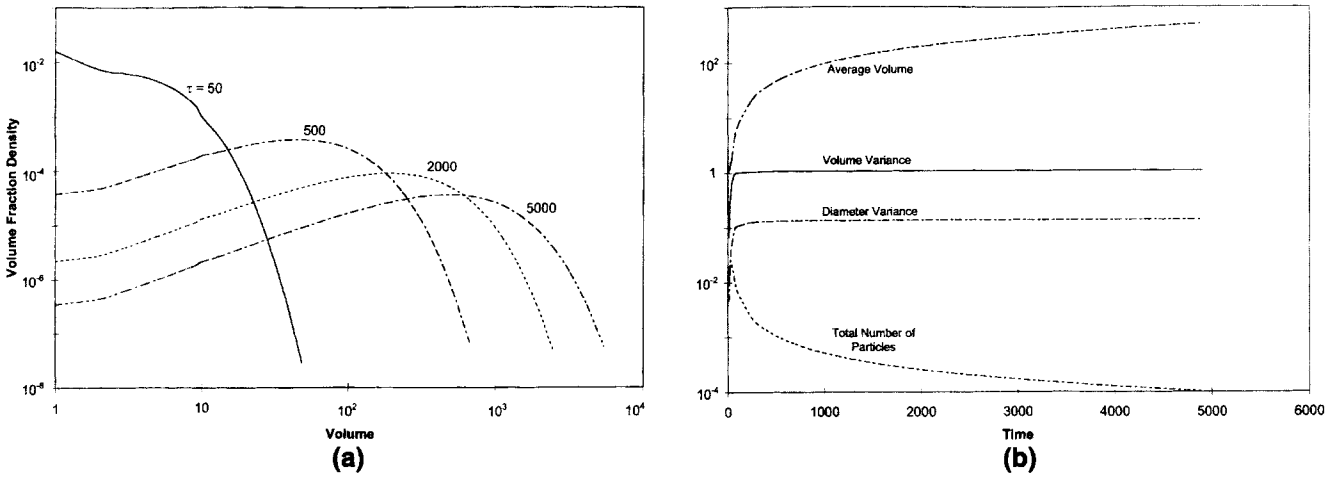

Figure 8. (a) Transient particle-size distributions; and (b) simple measures of the distribution for a system with no initial particles, Brownian aggregation, and a constant nucleation rate for a finite time $\sigma = 0.001$ for $\tau = 50$.

and the concentration of small particles decreases sharply and falls to very small values. This is a consequence of the high rate of aggregation of these small particles with all other particle sizes in the system, and due to their high concentration at the end of the nucleation period. The figure also shows that the distribution continues to quickly encompass larger particle sizes. However, as Figure 8b shows, the normalized variances increase and now approach a steady-state value. With the end of nucleation, the dispersed-phase system is undergoing Brownian aggregation with an initial condition specified by the distribution present at the end of the nucleation period.

Friedlander (1960, 1961) and coworkers (Swift and Friedlander, 1964) showed that the particle-size distribution eventually reaches a limiting self-similar form with any initial particle-size distribution undergoing Brownian aggregation. Size distributions at various times can be scaled with respect to the average particle size at that time to give curves identical to one another. They also evaluated this self-similar distribution and gave expressions for the asymptotes of the distribution. In terms of the normalized variances, the existence of self-similarity means that the normalized variances will reach a constant value after some time of aggregation. It needs to be emphasized that the self-similar distribution is achieved irrespective of the initial particle-size distribution.

In our case, the system evolves first toward the steady-state distribution obtained by Quon and Mockros, and then after nucleation stops it evolves toward the Brownian self-similar distribution calculated by Friedlander and coworkers. The steady-state values of σ_v and σ_d correspond to those for the self-similar distribution of a system undergoing Brownian aggregation.

Figure 9 shows another set of results for which the period of nucleation is longer than that for the case shown in Figure 8. Once again, during the nucleation period, the particle-size distribution evolves as discussed earlier and at the end of the nucleation period, particles up to approximately size 10 have reached a steady-state distribution. At the end of the nucle-

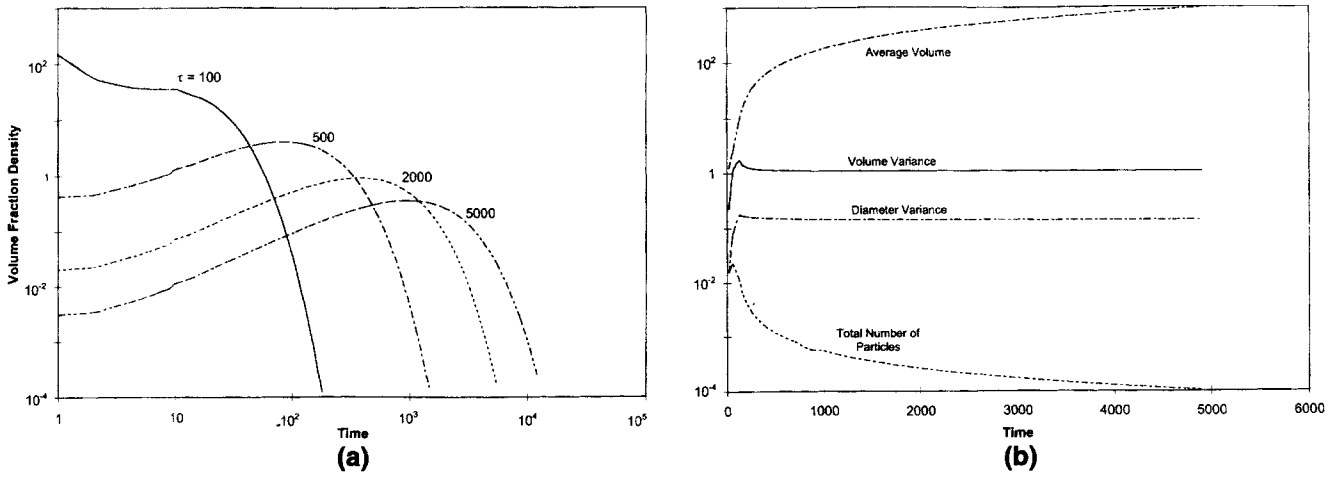

Figure 9. (a) Transient particle-size distributions, (b) simple measures of the distribution for a system with no initial particles, Brownian aggregation, and a constant nucleation rate for a finite time $\sigma = 0.001$ for $\tau = 100$.

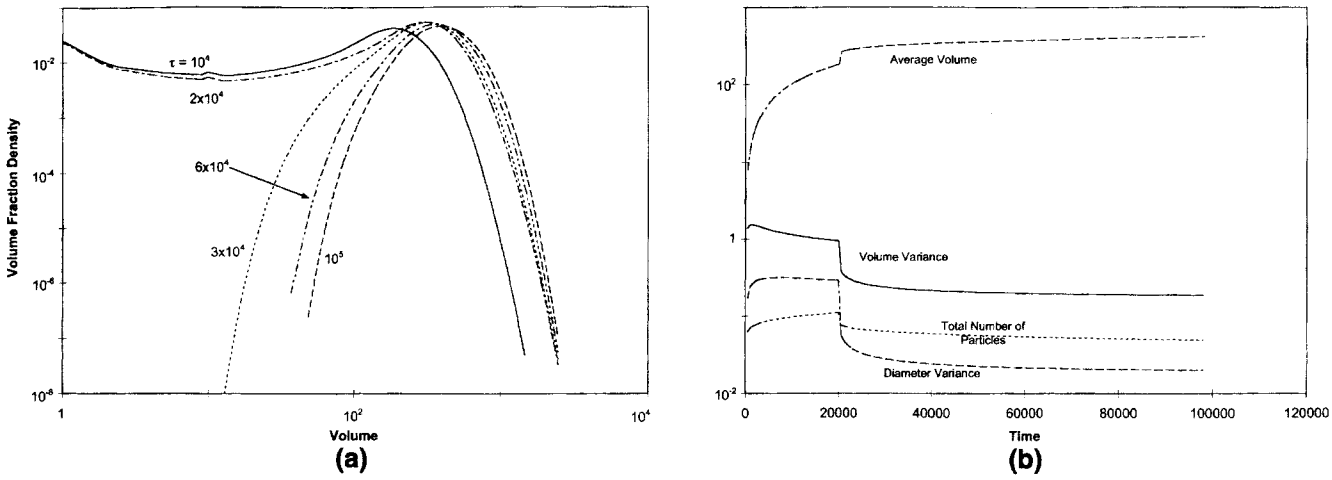

Figure 10. (a) Transient particle-size distributions, (b) simple measures of the distribution for a system with no initial particles, aggregation with DLVO interactions, and a constant nucleation rate for a finite time $\sigma = 0.001$ for $\tau = 20{,}000$.

ation period, the particle-size distributions are broad. The evolution of the particle-size distributions after cessation of nucleation, as shown in Figure 9a, show similar features to those discussed earlier. In this case, however, the values of σ_v and σ_d are higher than the corresponding values for the self-similar distribution and Figure 9b shows that the normalized variances monotonically decrease to the values corresponding to the self-similar distribution after nucleation stops.

"DLVO" Aggregation. Figure 10 shows typical results on the effect of stopping nucleation with DLVO interactions. While results are shown for a nucleation rate, similar results are obtained in calculations with other nucleation rates. Due to the reasonably high aggregation rate of the small particles with all particle sizes present in the system, these particles rapidly aggregate with other particles and quickly reduce to very low concentrations. The very slow aggregation rates of the large particles with one another makes the distribution grow very slowly to larger sizes. Figure 10b shows that the average particle size rapidly increases due to the disappearance of the small particles when nucleation stops. The volume and diameter variances also decrease sharply soon after nucleation stops and then slowly decrease as aggregation continues. Figure 11 shows that, independent of the duration of the nucleation period, the normalized variances attain a similar value if sufficient time is allowed for aggregation after nucleation stops. However, the figure also shows that the average particle size is strongly affected by the extent of nucleation with larger particles obtained by continuation of aggregation if the duration of nucleation is longer. This result suggests that one can tune the aggregate size without deteriorating the dispersity of the size distribution by suitable manipulation of the nucleation period.

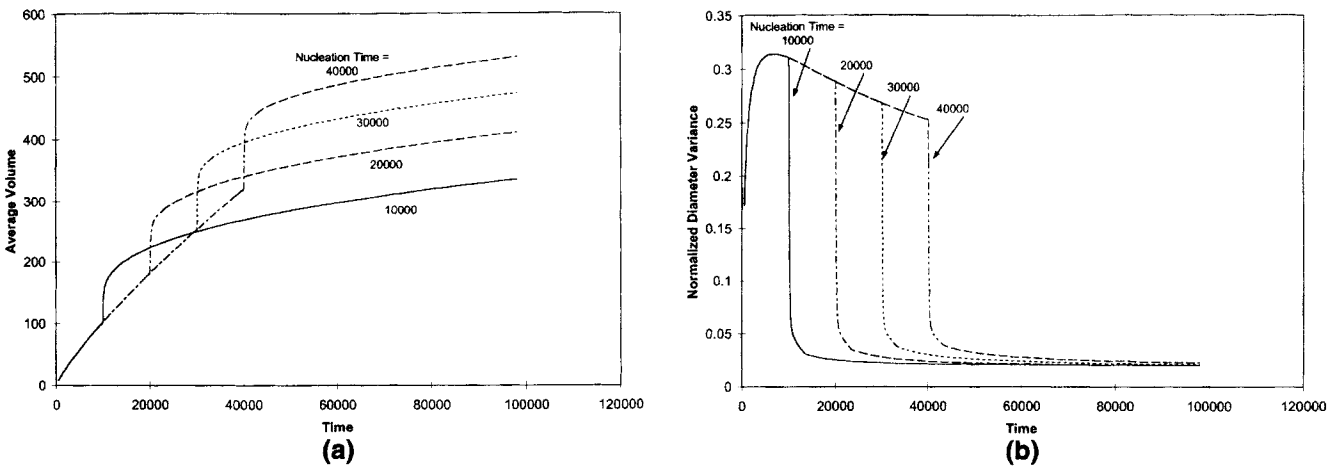

Figure 11. Evolution of the (a) average volume, (b) normalized diameter variance for a system with no initial particles, aggregation with DLVO interactions, and a constant nucleation rate for various fixed times.

Illustrates that the average size can be tuned without deteriorating the spread of the distribution.

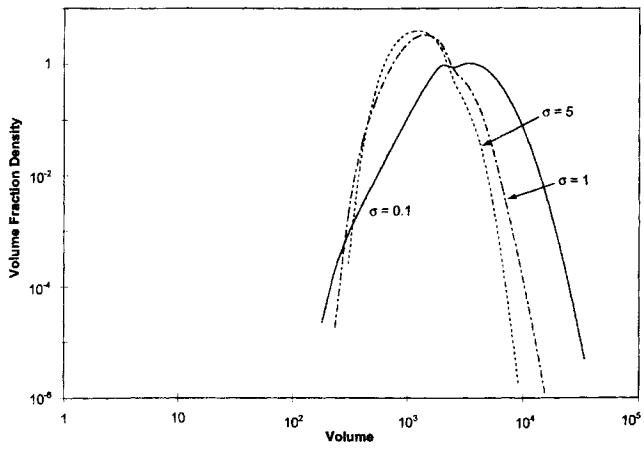

Figure 12. Particle-size distribution long after the end of the nucleation period for various nucleation rates and a fixed total amount of nucleation.

In this case, higher nucleation rates give smaller average particle sizes and sharper distributions.

Single and double nucleation periods

The previous sections show that nucleation with Brownian aggregation does not lead to a sharp particle-size distribution; so, in the following sections we will only consider aggregation with attractive and repulsive forces. We will investigate both "finite nucleation" and "double nucleation" keeping the same total yield (which, since we neglect growth, corresponds to the same total amount of nucleation).

Single Nucleation Period, Varying Nucleation Rate. In many colloid synthesis procedures, a fixed concentration of precursor material is used and the reaction (and nucleation) rate is varied by changing some other process variable (such as pH, temperature). We have simulated such a system by considering the effect of nucleation rate on the particle-size distribution for a fixed total amount of nucleation S (that is, for a fixed $S = \int_0^{\tau_{stop}} \sigma d\tau = \sigma\tau$ for constant nucleation). For a given nucleation rate, particles are allowed to nucleate for a time τ, after which nucleation is stopped and the particles are allowed to aggregate for some more time. Figure 12 shows the particle-size distributions at a fixed total amount of nucleation long after nucleation has stopped for three different nucleation rates. The figure shows that a higher nucleation rate leads to a smaller average particle size, but also decreases the spread of the distribution. This contrasts strongly with continuous nucleation results where a higher nucleation rate leads to larger particles (at a given time).

Double Nucleation Period, Varying Nucleation Time. In some colloid synthesis procedures, a bimodal particle-size distribution is occasionally observed. It has been speculated that the origin of this bimodal distribution is due to a second period of nucleation long after the first "instantaneous" nucleation. It is reasoned that the independent growth of this second set of nuclei leads to the bimodal distribution. This will certainly be the case if the second nucleation rate is too fast. However, here we show simulations indicating that this will not *always* be the case. If the second nucleation rate is sufficiently slow, new nuclei can aggregate with pre-existing large aggregates, maintaining the monodispersity. We have simulated this second nucleation process by assuming a nucleation profile as follows: (1) nucleation at a constant rate from $\tau = 0$ to $\tau = \tau_{pe}$; (2) no nucleation between $\tau = \tau_{pe}$ and $\tau = \tau_{ss}$, and (3) constant nucleation at the same rate as in stage (1) from $\tau = \tau_{ss}$ to $\tau = \tau_{se}$.

Figure 13 shows the evolution of the particle-size distribution when nucleation occurs between $\tau = 0$ and $\tau = 10{,}000$ and between $\tau = 50{,}000$ and $\tau = 60{,}000$. During the first nucleation period and the subsequent period with no nucleation, the evolution is identical to that discussed in the section on "DLVO" aggregation. Larger particles are slowly formed during the nucleation period; when nucleation stops, the small particles rapidly disappear due to their relatively high aggregation rate. The figure shows that soon after the second period of nucleation begins, the concentration of small particles increases. This indicated that the rate of nucleation is higher than the rate at which these particles can aggregate with the existing particle sizes. However, comparison of the particle-size distribution at the end of nucleation for different nucleation profiles shows that, for a given total amount

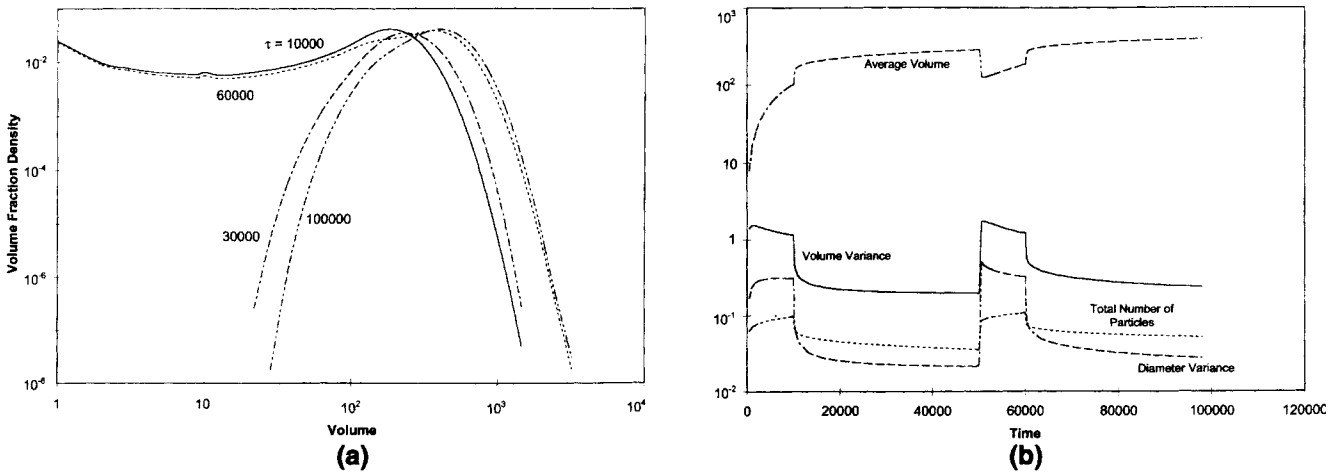

Figure 13. (a) Transient particle-size distributions; (b) simple measures of the distribution for a system with no initial particles, aggregation with DLVO interactions, and a constant nucleation rate over two time periods.

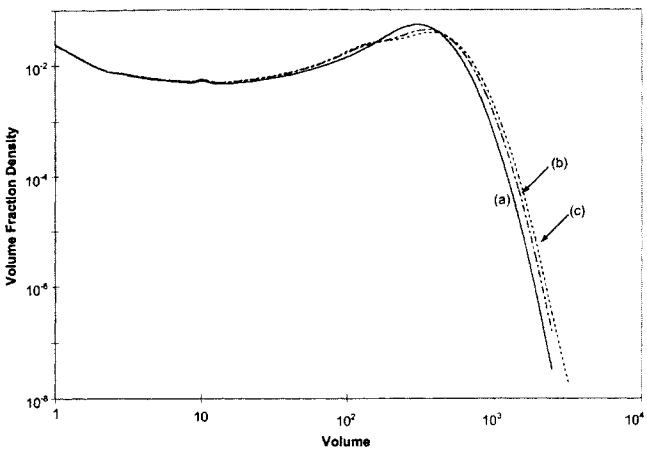

Figure 14. Particle-size distribution at the end of nucleation for a fixed total amount of nucleation and three different nucleation profiles, showing a minor effect of the nucleation profile on the size distribution.

(a) Continuous nucleation up to $\tau = 20{,}000$; (b) nucleation up to $\tau = 10{,}000$ and between $\tau = 30{,}000$ and $\tau = 40{,}000$; and (c) nucleation up to $\tau = 10{,}000$ and between $\tau = 50{,}000$ and $\tau = 60{,}000$.

of nucleation, the nucleation profile does not have a strong effect on the distribution. Figure 14 shows the distribution at the end of nucleation for three different nucleation profiles: (a) nucleation from $\tau = 0$ to $\tau = 10{,}000$ and from $\tau = 30{,}000$ to $\tau = 40{,}000$; (b) nucleation from $\tau = 0$ to $\tau = 10{,}000$ and from $\tau = 50{,}000$ to $\tau = 60{,}000$; and (c) continuous nucleation from $\tau = 0$ to $\tau = 20{,}000$. The figure shows only minor differences in the three distributions, particularly in light of the wide variation in nucleation profiles. The figure shows that the sharpest distribution is obtained with continuous nucleation, while giving more time for aggregation before the second nucleation gives a slightly broader distribution. This casts doubt on the view that a second nucleation will necessarily lead to a bimodal distribution. If the second nucleation is slow enough, the process can maintain monodispersity. For a given nucleation rate though, the distribution is strongly influenced by the total amount of nucleated particles.

Conclusions

We have studied the effects of nucleation on an aggregating colloidal dispersion. For a dispersion undergoing Brownian aggregation, a constant nucleation rate leads to a steady state in the number density of small particles and a continuously broadening distribution. On cessation of nucleation, the dispersion evolves to a broad, self-similar distribution.

The presence of interparticle attractive and repulsive forces changes the particle aggregation rate function and leads to interesting consequences for the particle-size distribution. We find that, at a fixed time, a higher nucleation rate will lead to larger average particle sizes and a much sharper distribution. We also find that, by varying the duration of nucleation at a fixed nucleation rate, and with continued aggregation after the cessation of nucleation, one might be able to tune the average particle volume without any deterioration in the spread of the distribution. For a fixed total amount of nucleation, a higher nucleation rate will lead to smaller particles and a sharper distribution. When nucleation occurs in multiple steps, one need not always observe a multimodal distribution. We have shown cases where multistep nucleation events can produce monodisperse particle-size distribution almost as narrow as single nucleation events.

Acknowledgments

We would like to thank Prof. D. Ramkrishna and Dr. Sanjeev Kumar (now at Indian Institute of Science, Bangalore) of Purdue University for many fruitful discussions and for providing us the computer program to do the calculations. We also acknowledge the financial support from NSF grant CTS9058387, and the resources of the Minnesota Supercomputer Institute.

Literature Cited

Bogush, G. H., and C. F. Zukoski, "Studies of the Kinetics of the Precipitation of Uniform Silica Particles Through the Hydrolysis and Condensation of Silicon Alkoxides," *J. Colloid Interf. Sci.*, **142**, 1 (1991a).

Bogush, G. H., and C. F. Zukoski, "Uniform Silica Particle Precipitation: An Aggregation Growth Model," *J. Colloid Interf. Sci.*, **142**, 19 (1991b).

Friedlander, S. K., "Similarity Considerations for the Particle-Size Spectrum of a Coagulating, Sedimenting Aerosol," *J. Meteor.*, **17**, 479 (1960).

Friedlander, S. K., "Theoretical Considerations for the Particle Size Spectrum of the Stratospheric Aerosol," *J. Meteor.*, **18**, 753 (1961).

Gelbard, F., and J. H. Seinfeld, "Numerical Solution of the Dynamic Equation for Particulate Systems," *J. Comput. Phys.*, **28**, 357 (1978).

Gelbard, F., and J. H. Seinfeld, "Exact Solution of the General Dynamic Equation for Aerosol Growth by Condensation," *J. Colloid Interf. Sci.*, **68**, 173 (1979a).

Gelbard, F., and J. H. Seinfeld, "The General Dynamic Equation for Aerosols: Theory and Application to Aerosol Formation and Growth," *J. Colloid Interf. Sci.*, **68**, 363 (1979b).

Hamaker, H. C., "The London-van der Waals Attraction Between Spherical Particles," *Physica*, **4**, 1058 (1937).

Hogg, R., T. W. Healy, and D. W. Fuerstenau, "Mutual Coagulation of Colloidal Dispersions," *Trans. Farad. Soc.*, **62**, 1638 (1966).

Kumar, S., and D. Ramkrishna, "On the Solution of Population Balance Equations by Discretization: I. A Fixed Pivot Technique," *Chem. Eng. Sci.*, **51**, 1311 (1996).

LaMer, V. K., and R. H. Dinegar, "Theory, Production and Mechanism of Formation of Monodispersed Hydrosols," *J. Amer. Chem. Soc.*, **72**, 4847 (1950).

Lee, K. T., J.-L. Look, M. T. Harris, and A. V. McCormick, "Assessing Extreme Models of the Stöber Synthesis Using Transients Under a Range of Initial Compositions," *J. Colloid Interf. Sci.*, **194**, 78 (1997).

Look, J.-L., G. H. Bogush, and C. F. Zukoski, "Colloidal Interactions During the Precipitation of Uniform Submicrometre Particles," *Farad. Discuss. Chem. Soc.*, **90**, 345 (1990).

Matsoukas, T., and E. Gulari, "Dynamics of Growth of Silica Particles from Ammonia-Catalyzed Hydrolysis of Tetra-ethyl-orthosilicate," *J. Colloid Interf. Sci.*, **124**, 252 (1988).

Matsoukas, T., and E. Gulari, "Monomer-Addition Growth with a Slow Initiation Step: A Growth Model for Silica Particles from Alkoxides," *J. Colloid Interf. Sci.*, **132**, 13 (1989).

Matsoukas, T., and E. Gulari, "Self-Sharpening Distributions Revisited—Polydispersity in Growth by Monomer Addition," *J. Colloid Interf. Sci.*, **145**, 557 (1991).

McMurry, P. H., and S. K. Friedlander, "New Particle Formation in the Presence of an Aerosol," *Atmos. Environ.*, **13**, 1635 (1979).

McMurry, P. H., "New Particle Formation in the Presence of an Aerosol: Rates, Time Scales, and Sub-0.01 μm Size Distributions," *J. Colloid Interf. Sci.*, **95**, 72 (1983).

Mockros, L. F., J. E. Quon, and A. T. Hjelmfelt, "Coagulation of a Continuously Reinforced Aerosol," *J. Colloid Interf. Sci.*, **23**, 90 (1967).
Ohshima, H., "Effective Surface Potential and Double-Layer Interaction of Colloidal Particles," *J. Colloid Interf. Sci.*, **174**, 45 (1995).
Peterson, T. W., F. Gelbard, and J. H. Seinfeld, "Dynamics of Source-Reinforced, Coagulating, and Condensing Aerosols," *J. Colloid Interf. Sci.*, **63**, 426 (1978).
Quon, J. E., and L. F. Mockros, "The Equilibrium Size Distribution of an Aerosol Continually Reinforced with Particles," *Int. J. Air Water Poll.*, **9**, 279 (1965).
Ramabhadran, T. E., T. W. Peterson, and J. H. Seinfeld, "Dynamics of Aerosol Coagulation and Condensation," *AIChE J.*, **22**, 840 (1976).
Ramkrishna, D., "The Status of Population Balances," *Rev. Chem. Eng.*, **3**, 49 (1985).
Ramkrishna, D., A. N. Sathyagal, and G. Narsimhan, "Analysis of Dispersed-Phase Systems: Fresh Perspective," *AIChE J.*, **41**, 35 (1995).
Rao, N. P., and P. H. McMurry, "Nucleation and Growth of Aerosol in Chemically Reacting Systems," *Aerosol Sci. Tech.*, **11**, 120 (1989).
Smoluchowski, M. V., "Drei Vorträge über Diffusion, Brownsche Molekularbewegung und Koagulation von Kolloidteilchen," *Physik. Z.*, **17**, 585 (1916).
Swift, D. L., and S. K. Friedlander, "The Coagulation of Hydrosols by Brownian Motion and Laminar Shear Flow," *J. Colloid Interf. Sci.*, **19**, 621 (1964).
Verwey, E. J. W., and J. Th. G. Overbeek, "Theory of the Stability of Lyophobic Colloids, Elsevier, New York (1948).
Warren, D. R., and J. H. Seinfeld, "Nucleation and Growth of Aerosol from a Continuously Reinforced Vapor," *Aerosol Sci. Tech.*, **3**, 135 (1984).

Manuscript received June 23, 1997, and revision received July 28, 1998.